PHYSICAL REVIEW LETTERS

Doping Controlled Superconductor-Insulator Transition in $Bi_2Sr_{2-x}La_xCaCu_2O_{8+\delta}$

Seongshik Oh,* Trevis A. Crane, D. J. Van Harlingen, and J. N. Eckstein

Department of Physics, University of Illinois, Urbana, Illinois 61801, USA
(Received 20 September 2005; published 14 March 2006)

We show that the doping-controlled superconductor-insulator transition (SIT) in a high critical temperature cuprate system ($Bi_2Sr_{2-x}La_xCaCu_2O_{8+\delta}$) exhibits a fundamentally different behavior than is expected from conventional SIT. At the critical doping, the sheet resistance seems to diverge in the zero-temperature limit. Above the critical doping, the transport is universally scaled by a two-component conductance model. Below, it continuously evolves from weakly to strongly insulating behavior. The two-component conductance model suggests that a collective electronic phase-separation mechanism may be responsible for this unconventional SIT behavior.

Since the late 1980s, the superconductor-insulator transition has been intensively studied both experimentally [1–4] and theoretically [5–9] in homogeneously disordered two-dimensional (2D) thin films. These studies suggest that there exists a defect-scattering dominated metallic (that is, resistance being temperature-independent) state with a finite zero-temperature critical sheet resistance at the transition from superconducting to insulating behavior. Samples with sheet resistance less than this critical value are superconducting as $T \to 0$, otherwise they are insulating.

High-T_c cuprates (HTCs) are a quasi-2D system, and magnetic field [10,11] or doping control [12–14] can continuously transform superconducting cuprates into insulators as in the conventional SIT. In the case of doping-controlled SIT, there exists a common feature for all cuprates in the temperature dependence of the in-plane resistance. For doping levels much higher than the critical doping, the resistance monotonically decreases as a function of decreasing temperature and drops to zero below a superconducting transition temperature. For doping levels below the critical doping, the resistance first decreases as a function of decreasing temperature at high temperatures, reaches a minimum at an intermediate temperature, and then it starts to increase as the temperature is further reduced. However, for a small range of doping levels just above the critical doping, the temperature dependence of the resistance is composed of three regions [10–13]. As a function of decreasing temperature, the resistance first decreases at high temperatures, reaches a minimum at an intermediate temperature, starts to increase at lower temperatures until it reaches a local maximum, and then it drops to zero resistance below the superconducting transition temperature. Although such a reentrant behavior is universally observed in almost all underdoped cuprates [10–13], its origin or significance has not attracted much attention so far.

In this Letter, however, we report the results of a doping-controlled SIT study with an unprecedented level of detail, and we find that important physics has been hidden in this phenomenon. First of all, the sheet resistance tends to diverge as $T \to 0$ at the critical doping, contrary to the common notion of finite critical sheet resistance not only in conventional disordered metals [1–4] but also in cuprates [12,13]. Above the critical doping, the reentrant behavior is well described by a two-component scaling function composed of a weakly insulating phase and a superconductive-fluctuating phase. This model is consistent with the widely predicted and observed electronic phase-separation mechanism driven by carrier-carrier correlations [15–19]. We attribute the observed divergence of the critical sheet resistance to this phase-separation phenomenon. Below the critical doping, the transport continuously evolves into two-dimensional variable-range hopping.

For a detailed doping-controlled SIT study, we have grown a 40 molecular layer of $Bi_2Sr_{1.56}La_{0.44}CaCu_2O_{8+\delta}$ (Bi2212:La = 0.44) film by ozone-assisted molecular beam epitaxy and varied its doping level in the vicinity of the SIT in small steps (smaller than 0.001 holes per Cu in doping) using precise and reversible oxygen control [20]. Each curve in Fig. 1 is obtained after a few minutes of either vacuum ($\sim 10^{-8}$ Torr) or ozone ($\sim 10^{-6}$ Torr) annealing at $\sim 400\,^\circ$C. Figure 1 shows sheet resistance (R_S) defined per CuO_2 bilayer versus temperature (T) curves very near the SIT. Overall, there exist two temperature
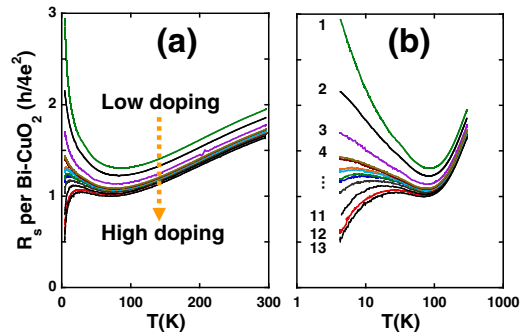

FIG. 1 (color online). Doping-controlled SIT over a very small range of doping levels. (a) and (b) are the same data plotted on different horizontal scales. Note that each curve is indexed by a number 1 through 13 in the order of increasing doping.

regions in Fig. 1(a). Each curve reaches a local minimum at a characteristic temperature T_{min} near 80 K. Above T_{min}, all the curves exhibit metallic behavior ($dR/dT > 0$), and doping simply provides a temperature-independent shift with respect to one another. However, below T_{min} all the curves switch to an insulating behavior ($dR/dT < 0$), diverging away from each other as temperature decreases.

When the temperature is further reduced, the temperature dependence of the resistance either switches to a metallic behavior ($dR/dT > 0$) when the doping exceeds a critical value or remains insulating. This is more easily seen in Fig. 1(b) where we plot resistance versus log$T$. We interpret the change to metallic behavior as the onset of superconducting fluctuations and expect these samples will eventually become superconducting at low temperatures since they are obtained by incrementally reducing the doping level of a sample which shows a superconducting transition above 4.2 K. The samples which exhibit superconducting fluctuations show a resistance peak R_p at a temperature T_p below which the resistance drops. Conversely, samples which do not show a peak in resistance are on the insulating side of the SIT.

In conventional superconductors, the temperature dependence of resistance just above the superconducting transition temperature is generally flat due to temperature-independent defect scattering [1,4]. However, emergence of a superconducting transition from an insulating temperature dependence, which we call reentrant behavior, has been observed in granular superconductors, where superconducting islands are embedded in an insulating background [21–23]. In such a case, even when the high-temperature dependence shows insulating behavior due to Coulomb charging energy, if the intergrain tunneling energy and the Josephson coupling energy overcome the Coulomb energy at reduced temperatures, a superconducting transition can occur from an insulating normal phase. We propose that the insulating normal-state temperature dependence, which we see here even in superconducting samples, is of a similar origin. Although HTCs are structurally homogeneous, theories have predicted that hole carriers may segregate into hole-rich and hole-poor islands at low doping due to strong carrier-carrier correlation effect [24–27], and scanning-tunneling experiments have verified that such granular electronic states prevail in underdoped HTCs [18,19].

According to this phase-separation scenario, the reentrant behavior observed for doping levels above the critical value can be qualitatively understood. At temperatures above T_{min}, strong thermal fluctuations wash out any phase-separation mechanism, leaving only metallic behavior. Below T_{min}, however, phase separation occurs such that hole-rich (presumably superconducting) islands are formed inside a hole-poor (presumably insulating) background. In this case, the resistance is dominated by the insulating background until superconducting islands start to couple with each other at lower temperatures, ultimately

giving rise to a global superconducting transition. Although such reentrant behavior is universally observed in almost all underdoped HTC systems [10–13,28], its origin has not been well known. Below, using a two-component conductance model, we present a quantitative analysis supporting the phase-separation as the main mechanism behind this reentrant behavior.

A key finding of our work is that the bottom 8 curves (curves 6 through 13) from Fig. 1(b), which show resistance peaks above 4.2 K, can be rescaled by dividing the temperature by T_p and the resistance by R_p. When this is done, the low-temperature parts of the curves overlap nicely as shown in Fig. 2(a). This suggests that there exists a single scaling function $r = r(t)$, where $r \equiv R/R_p$ and $t \equiv T/T_p$, which describes the transition from insulating to superconducting temperature dependence for all of the superconducting curves. One can find a well-fitting scaling function, $r(t)$, using a simple two-component conductance model, where the total conductance, $g(t) = r(t)^{-1}$, is due to two contributions and is given by $g(t) = At^q + B\frac{t_c}{t - t_c}$ with $A = 0.881$, $q = 0.145$, $B = 1.72$, and $t_c (\equiv T_c/T_p) = 0.065$ found as the parameters leading to the best fit of the data. Here T_c represents the superconducting critical temperature, below which the resistance of the sample turns
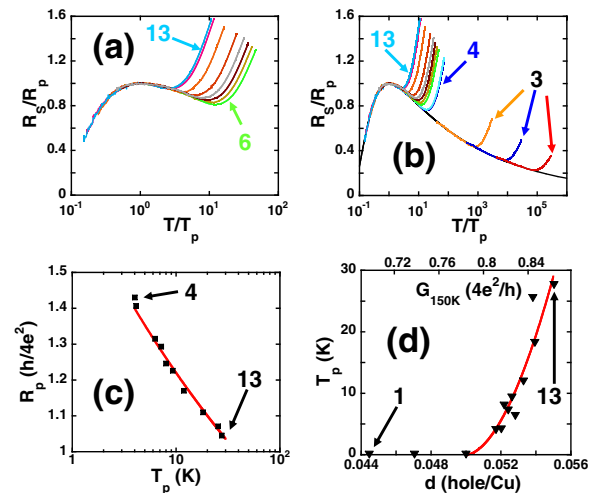

FIG. 2 (color online).   Scaling of superconducting curves. Each index represents the corresponding curve from Fig. 1(b). (a) Rescaled plot of curves 6–13 from Fig. 1(b). (b) The two-component scaling function plotted together with curves 3–13. Curves 6–13 are used to obtain the scaling function. Curves 4–5 are fit to the obtained scaling function with T_p and R_p as the fitting parameters. As for curve 3, any choice of T_p below ~0.5 K gives reasonably good fitting; three curves with $T_p = 0.1$ K, 0.01 K, and 0.001 K are shown from left to right as examples. (c) R_p vs T_p for the 10 superconducting curves (4–13). The solid line represents the best fitting for the 8 measured data points (curves 6–13), which corresponds to $R_p = 1.72 T_p^{-0.149}$. (d) T_p vs doping. Conductance at 150 K is also shown on the top axis. The solid line, $T_p = 4.02 \times 10^5 \times (d - d_c)^{1.8}$, is the best fitting for $d > d_c$.

zero. Since $g(1) = 1$ and $g'(1) = 0$ by the definition of T_p, among the four parameters only two (for example, q and t_c) are independent, and the other two can be obtained from $A = [1 + q(1 - t_c)]^{-1}$ and $B = Aq(1 - t_c)^2$. The two independent model parameters, q and t_c, determine the relative insulating and superconductive-fluctuating transport contributions, respectively, as described below.

Both terms of this two-component conductance formula correspond to physically identifiable conductance channels and this is consistent with the above-mentioned phase-separation mechanism. The first term represents the conductance of 2D weakly insulating normal carriers from the hole-poor background, while the second is due to the conductance of fluctuating superconducting pairs from the hole-rich islands, similar in form to the 2D superconducting fluctuations treated by Aslamasov and Larkin (AL) [29]. In AL theory, the fluctuation contribution, however, is not referenced to any material property and is scaled only by $4e^2/h$. In our case, since $1/R = g(t)/R_p$, the contribution of this term to the overall conductance is scaled by $1/R_p$ which is strongly dependent on doping.

The two-component scaling function determined from curves 6–13 in Fig. 2(a) is plotted in Fig. 2(b) together with curves 3–13. Curves 4 and 5 can be nicely fit to the scaling function with T_p values less than 4.2 K and corresponding R_p values. Curves 1 and 2 cannot be fit to the scaling function for any choice of T_p and R_p values. Curve 3 can be scaled with a range of R_p and T_p pairs in which T_p can take any values between 0 and $\sim$0.5 K. In order to show this, we have selected three representative values, 0.1 K, 0.01 K, and 0.001 K for T_p and presented the corresponding fitting curves in Fig. 2(b). All three curves are equally well fit to the scaling function even if their T_p values are orders of magnitude different with one another. This means that the doping level, d, in curve 3 is very near the $T_c = 0$ transition value, but it is impossible to know whether it is exactly zero or just very nearly zero.

The temperature dependence corresponding to the critical doping, d_c, can be obtained by taking the limit of the scaling function as $T_c \propto T_p \to 0$, which corresponds to $R = 1.14 R_p (T_p/T)^{0.145}$. Once the relationship between R_p and T_p is known, temperature dependence at critical doping can be determined. Our two-component conductance model does not give any *a priori* information about how T_p and R_p are related, and they should be obtained from R versus T curves. Figure 2(c) shows the result of this, and we find $R_p \approx 1.72 \times T_p^{-0.149}$ as the best fit for the 8 data points (curves 6–13) of R_p versus T_p. Values of R_p and T_p for the other two (curves 4 and 5) with $T_p < 4.2$ K are obtained by fitting the corresponding R versus T curves to the scaling function and are plotted for comparison as well. Using this relationship, the temperature dependence at critical doping reduces to $R = 1.96 \times T^{-0.145} T_p^{\alpha}$, where $\alpha = -0.004$.

The exact value of α is significant because $\alpha = 0$ implies that there exists an asymptotic critical-doping tem-

perature dependence to which $R(T)$ tends as the doping approaches d_c from the superconducting side. Since the error in determining the exponent is close to 0.01, we believe the obtained value is effectively zero. If α were not zero, then as $T_c \to 0$, R would tend either toward zero or infinity for all temperatures depending on the sign of α, either of which is unphysical. Since we find $\alpha \sim 0$, we believe our scaling function and empirical relationship between R_p and T_p provide a well-behaved limiting form as T_c goes to zero.

This result is interesting because it suggests that, for the doping-controlled SIT, the critical temperature dependence is insulating ($dR/dT < 0$), and a zero-temperature critical sheet resistance does not exist. This is in direct contrast to the conventional picture of the SIT, according to which a temperature-independent and finite sheet resistance exists at a critical value of the control parameter [1–4,12,13]. Although this conclusion needs to be verified by further studies at lower temperatures, we believe that it would remain unchanged, because the transport data do not show any sign of deviation from the two-component scaling form in the temperature range we have studied.

Making use of the normal-state conductance, G, which is monotonically related to the doping level as shown in Fig. 1, it is possible to estimate the doping level, d, of each curve, since within a reasonable approximation G must be proportional to d. Assuming that d of curve 3 is the critical value, d_c and taking 0.05 hole/Cu, the widely accepted value for the critical doping [30], as the critical value, we have converted G at 150 K into d in Fig. 2(d) and presented T_p as a function of the doping level. Since $T_c (\propto T_p)$ is the energy scale that governs transport on the superconducting side and renormalization scaling predicts $T_c \propto |d - d_c|^{\nu z}$ [6], a power-law relationship is expected between T_p and doping. From Fig. 2(d), the estimated critical exponent is $\nu z = 1.8 \pm 0.3$.
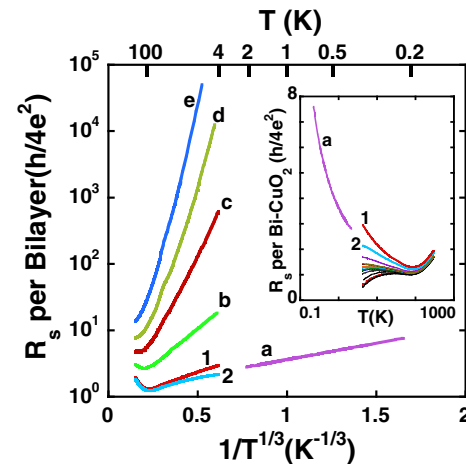

FIG. 3 (color online). R_S vs $1/T^{1/3}$ for insulating doping levels. Linearity in this plot implies 2D-VRH. Curves 1 and 2 from Fig. 1 are reproduced for comparison. Inset shows how curve a compares with other curves from Fig. 1.
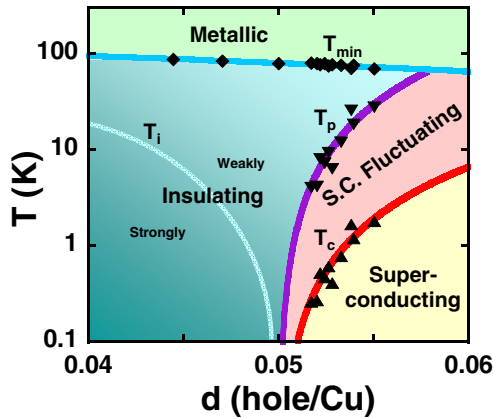
FIG. 4 (color online). (T, d) phase diagram near the critical doping. T_p and $T_{\min}$ are determined by the resistance data, and T_c is evaluated as $0.065 \times T_p$ according to the scaling analysis. Fitting curves for each of these crossover temperatures are plotted as well. Unlike other crossover temperatures, T_i is only marginally defined in our experiment.

Transport on the insulating side of the SIT is shown in Fig. 3, where curves 1 and 2 from Fig. 1 are reproduced. We also measured the temperature dependence of the sheet resistance for a barely insulating sample between 2 and 0.2 K; this is labeled curve a. For curves a and b, the resistance is well described by 2D variable-range hopping (VRH), where $R(T) = R_0 \exp(T_0/T)^{1/3}$ [31,32]. Here $T_0 = 10/k_B \xi^2 N(E_F)$ where $N(E_F)$ is the density of states at the Fermi level, and ξ is the characteristic size of the localized states between which hopping occurs. In our data T_0 tends to zero as the doping level approaches the critical doping from the insulating side. Curve 2 is better fit by a power law within the measured temperature range. Curve 1 tends to deviate from a high-temperature power law toward a low-temperature 2D-VRH dependence. Even curve 2 may take a 2D-VRH form at very low temperatures. This observation suggests the existence of a crossover temperature, T_i, at which a weakly insulating (power-law-dependent) high-temperature behavior transforms into a strongly (quasiexponential such as 2D-VRH) insulating low-temperature one. In the other extreme, when T_0 gets very large and ξ very small, the transport starts to diverge faster than is expected by VRH, which is the case for curves c, d, and e.

All the above observations can be summarized into a (T, d) phase diagram shown in Fig. 4. It is composed of metallic, insulating, superconductive fluctuating (i.e., local superconducting), and global superconducting regions divided by three crossover temperatures, $T_{\min}$, T_p, and T_c. The insulating region can again be divided into weakly and strongly insulating regions by T_i. Especially, our analysis suggests that the phase separation phenomenon results in the reentrant behavior for $0.050 \sim 0.058$ (hole/Cu) doping levels and the weakly insulating $T \rightarrow 0$ behavior at the critical doping, 0.050 (hole/Cu).

*Email address: soh4@uiuc.edu
Present address: National Institute of Standards and Technology, Boulder, CO 80305, USA.
[1] D. B. Haviland, Y. Liu, and A. M. Goldman, Phys. Rev. Lett. **62**, 2180 (1989).
[2] N. Markovic *et al.*, Phys. Status Solidi B **218**, 221 (2000).
[3] A. Yazdani and A. Kapitulnik, Phys. Rev. Lett. **74**, 3037 (1995).
[4] A. M. Goldman, Physica (Amsterdam) **18E**, 1 (2003).
[5] T. Pang, Phys. Rev. Lett. **62**, 2176 (1989).
[6] M. P. A. Fisher, G. Grinstein, and S. M. Girvin, Phys. Rev. Lett. **64**, 587 (1990).
[7] M. C. Cha and S. M. Girvin, Phys. Rev. B **49**, 9794 (1994).
[8] D. Das and S. Doniach, Phys. Rev. B **57**, 14 440 (1998).
[9] P. Phillips and D. Dalidovich, Science **302**, 243 (2003).
[10] Y. Ando *et al.*, Phys. Rev. Lett. **75**, 4662 (1995).
[11] S. Ono *et al.*, Phys. Rev. Lett. **85**, 638 (2000).
[12] K. Semba and A. Matsuda, Phys. Rev. Lett. **86**, 496 (2001).
[13] Z. Konstantinovic, Z. Z. Li, and H. Raffy, Physica (Amsterdam) **351C**, 163 (2001).
[14] T. Tamegai *et al.*, Jpn. J. Appl. Phys. **28**, L112 (1989).
[15] E. Sigmund and K. A. Müller, *Phase Separation in Cuprate Superconductors* (Springer-Verlang, Berlin, 1994).
[16] E. Dagotto, Rev. Mod. Phys. **66**, 763 (1994).
[17] S. A. Kivelson *et al.*, Rev. Mod. Phys. **75**, 1201 (2003).
[18] K. M. Lang *et al.*, Nature (London) **415**, 412 (2002).
[19] S. H. Pan *et al.*, Nature (London) **413**, 282 (2001).
[20] S. Oh, T. Di Luccio, and J. N. Eckstein, Phys. Rev. B **71**, 052504 (2005).
[21] Y. Shapira and G. Deutscher, Phys. Rev. B **27**, 4463 (1983).
[22] M. Ma and P. A. Lee, Phys. Rev. B **32**, 5658 (1985).
[23] E. Simánek, *Inhomogeneous Superconductors: Granular and Quantum Effects* (Oxford University Press, New York, 1994).
[24] L. P. Gor'kov and A. V. Sokol, JETP Lett. **46**, 420 (1987).
[25] V. I. Yukalov and E. P. Yukalova, Phys. Rev. B **70**, 224516 (2004).
[26] V. J. Emery, S. A. Kivelson, and H. Q. Lin, Phys. Rev. Lett. **64**, 475 (1990).
[27] V. J. Emery and S. A. Kivelson, Physica (Amsterdam) **209C**, 597 (1993).
[28] S. Komiya, H. D. Chen, S. C. Zhang, and Y. Ando, Phys. Rev. Lett. **94**, 207004 (2005).
[29] L. G. Aslamasov and A. I. Larkin, Phys. Lett. **26A**, 238 (1968).
[30] M. R. Presland *et al.*, Physica (Amsterdam) **176C**, 95 (1991).
[31] N. F. Mott, *Conduction in Non-Crystalline Materials* (Clarendon, Oxford, 1993).
[32] B. I. Shklovskii and A. L. Efros, *Electronic Properties of Doped Semiconductors* (Springer-Verlag, Berlin, 1984).